PAPER • **OPEN ACCESS**

Increasing N content in GaNAsP nanowires suppresses the impact of polytypism on luminescence

To cite this article: Mattias Jansson *et al* 2019 *Nanotechnology* **30** 405703

OPEN ACCESS
IOP Publishing
Nanotechnology

Nanotechnology **30** (2019) 405703 (7pp)
https://doi.org/10.1088/1361-6528/ab2cdb

Increasing N content in GaNAsP nanowires suppresses the impact of polytypism on luminescence

Mattias Jansson[1,5], Luca Francaviglia[2], Rui La[3], Roman Balagula[1], Jan E Stehr[1], Charles W Tu[3], Anna Fontcuberta I Morral[2,4], Weimin M Chen[1] and Irina A Buyanova[1,5]

[1] Department of Physics, Chemistry and Biology, Linköping University, SE-58183 Linköping, Sweden
[2] Laboratoire des Matériaux Semiconducteurs, Institut des Matériaux, Ecole Polytechnique Fédérale de Lausanne, 1015 Lausanne, Switzerland
[3] Department of Electrical and Computer Engineering, University of California, San Diego, La Jolla, CA 92093, United States of America
[4] Institute of Physics, Faculty of Basic Sciences, EPFL, 1015 Lausanne, Switzerland

E-mail: mattias.jansson@liu.se and irina.bouianova@liu.se

Received 2 April 2019, revised 15 May 2019
Accepted for publication 26 June 2019
Published 19 July 2019

Abstract

Cathodoluminescence (CL) and micro-photoluminescence spectroscopies are employed to investigate effects of structural defects on carrier recombination in GaNAsP nanowires (NWs) grown by molecular beam epitaxy on Si substrates. In the NWs with a low N content of 0.08%, these defects are found to promote non-radiative (NR) recombination, which causes spatial variation of the CL peak position and its intensity. Unexpectedly, these detrimental effects can be suppressed even by a small increase in the nitrogen composition from 0.08% to 0.12%. This is attributed to more efficient trapping of excited carriers/excitons to the localized states promoted by N-induced localization and also the presence of other NR channels. At room temperature, the structural defects no longer dominate in carrier recombination even in the NWs with the lower nitrogen content, likely due to increasing importance of other recombination channels. Our work underlines the need in eliminating important thermally activated NR defects, other than the structural defects, for future optoelectronic applications of these NWs.

Supplementary material for this article is available online

Keywords: nanowires, polytypism, dilute nitrides, stacking faults, twinning

(Some figures may appear in colour only in the online journal)

1. Introduction

III–V semiconductor nanowires (NWs) have recently drawn much attention due to their attractive physical properties, including a direct bandgap and high carrier mobilities [1–3], advantageous for electronic and optoelectronic applications. The growth in the NW geometry has numerous additional benefits, ranging from the ability to integrate III–V optoelectronic components with Si-based microelectronic devices to various ways to enhance device performance by utilizing the geometry itself [4–9]. For example, depending on the diameter, a nanowire naturally forms a light waveguide or a cavity, beneficial for lasing [4, 8], while a high surface-to-volume ratio in such structures significantly increases sensitivity of sensing [9].

[5] Authors to whom any correspondence should be addressed.

It has previously been demonstrated that growth of III–V materials in the NW geometry may introduce crystal phase changes not found in the bulk form of the crystals. Both III-arsenides and -phosphides, which have the zinc-blende (ZB) crystal structure in their bulk form, may form the wurtzite (WZ) crystal structure or other polytypes in NWs [10]. A combination of WZ and ZB phases, together with related stacking faults (SF) and rotational twin planes, is often observed within the same NW [11, 12]. This polytypism, accompanied by the presence of the SF and twins, affects the electronic structure and optical properties of the materials [12–18]. It was also shown that random ZB/WZ polytypism has detrimental effects on the electronic and optoelectronic properties of NWs, as rotational twin planes and SF may reduce carrier mobility and act as non-radiative (NR) recombination centers, respectively [19–23]. For any device application to be viable, this issue needs to be resolved. For this reason, many efforts have been made in the rather challenging task to grow single-phase crystalline NWs that are free of structural defects [24–30].

Among promising materials for electronic and optoelectronic applications is GaNAsP with a low N composition of up to a few atomic percent, which belongs to the family of dilute nitride alloys [31]. Dilute nitrides have a number of unusual fundamental physical properties, including giant bandgap bowing, as incorporation of 1% of nitrogen may reduce the bandgap energy by more than 100 meV [31]. Dilute nitrides also experience a splitting of the conduction band into two separate subbands, a feature that is promising for intermediate band solar cells [32, 33], and a reduced temperature dependence of the bandgap compared to other III–V materials [34]. Moreover, GaNAs structures exhibit several extraordinary spin properties, which may be utilized in future spintronic applications [35–38]. Quaternary dilute nitride GaNAsP NWs have recently been successfully grown [39] with nitrogen compositions up to 0.16%. They have been shown to primarily crystallize in the ZB phase, but with some rotational twin planes and SF, as well as small WZ inclusions [40]. However, effects of this polytypism on optical properties of these NWs remain hitherto unexplored. In this paper, we address this important issue using correlative cathodoluminescence (CL) and micro-photoluminescence (μPL) measurements. We first illustrate how polytypism affects the uniformity of the emission energy and intensity along single NWs. We then demonstrate how the addition of nitrogen in a controlled percentage enhances the uniformity of the NW emission by acting on the recombination dynamics. This strategy may help to tackle the effect of crystal defects on the optical properties of GaNAsP through a simpler yet effective approach in comparison with the direct engineering of the NW crystal structure.

2. Experimental details

The investigated GaNAsP NWs were grown by self-catalyzed plasma-assisted MBE on (111) Si substrates [39]. Thermally cracked PH_3 and AsH_3 were used as the source of As_2 and P_2, respectively, while Ga was supplied from a solid Ga source. Nitrogen was supplied from a N-plasma operating in the range of 200–250 W. The investigated NWs have the same P content of around 24%, whereas the nitrogen composition in the two samples is 0.08% and 0.12%, as estimated using the band anticrossing model [41, 42] (for full details, see supporting information, available online at stacks.iop.org/NANO/30/405703/mmedia). According to the performed scanning electron microscopy (SEM) measurements, the average NW length is 2 (1) μm for the [N] = 0.08 (0.12)% samples. Full details of the growth process are given in [39]. Structural properties of individual NWs, mechanically transferred to a C/Cu grid, were investigated using a FEI Tecnai G2 TF 20 UT transmission electron microscope. CL and μPL measurements were performed on single NWs transferred to Au or Si substrates. The CL data were acquired using the Rosa microscope from Attolight using a beam energy between 3 and 5 keV at temperatures of 8 and 300 K. μPL spectra were measured at 6 K using a confocal microscope (50X, 0.5 NA) coupled with a single grating spectrometer and a CCD camera. In the μPL experiments, the PL emission was excited by using either a 532 nm solid-state laser or a tunable Ti:Sapphire laser, where the latter was employed for μPL-excitation (μPLE) measurements. The size of the laser spot on the sample was estimated to be in the range of 0.8–2 μm, slightly increasing with increasing laser power. From this it is concluded that half or more of the NW volume is excited simultaneously during μPL (μPLE) measurements.

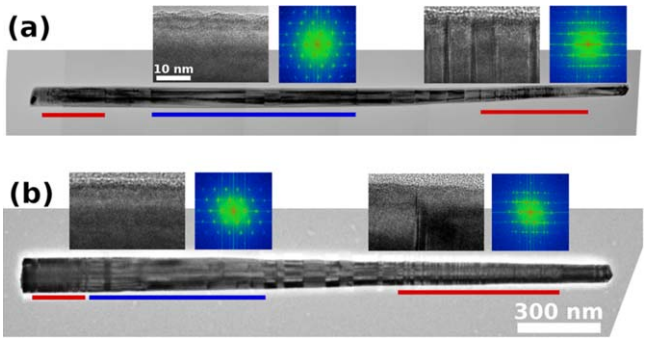

Figure 1. TEM images of representative GaNAsP NWs with [N] = 0.08% (a) and 0.12% (b). The regions marked by the red and blue lines have a high and low density of structural defects, respectively. The insets show high-magnification images of parts of these areas and the fast Fourier transformation of these images.

3. Results and discussion

Representative transmission electron microscopy (TEM) images of the studied NWs are shown in figures 1(a) and (b), respectively. In the overview images, numerous radial lines across the NWs can be seen, which are related to structural defects such as twin planes and SF commonly seen in III–V semiconductor NWs. Distributions of such structural defects are rather similar in both structures—the defect density is high near the tip and within the very bottom part of each NW, as marked by the red lines in the figure. Conversely, large areas

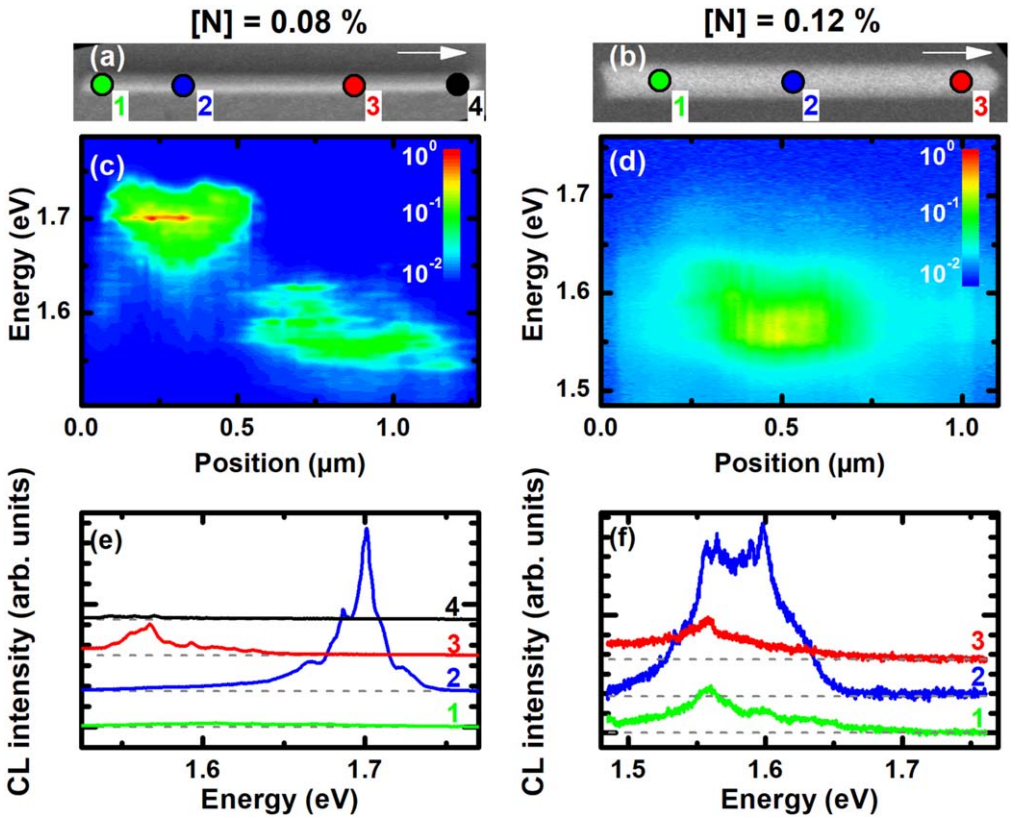

Figure 2. SEM images of representative GaNAsP NWs with [N] = 0.08% (a) and 0.12% (b), where the arrow indicates the growth direction. Spatial and spectral distributions of the CL emission measured at 8 K for the same NWs with [N] = 0.08% (c) and 0.12% (d), using an acceleration voltage of 3 and 5 kV, respectively, displayed in the logarithmic scale. The results are found to be insensitive to acceleration voltage. (e) And (f) CL spectra acquired from several spatial locations of the NWs as indicated in (a) and (b), respectively, displayed in the linear scale. The spectra are vertically offset, for clarity.

of the lower half of the NWs (marked by the blue lines) have a very low defect density, as shown by the high-resolution TEM images of these areas and the fast Fourier transformation of these images.

To investigate possible impacts of the revealed structural defects on the optical properties, spatially-resolved CL spectroscopy was performed on individual NWs. Figure 2 summarizes the results from these measurements for the GaNAsP NWs with [N] = 0.08% and 0.12%, of which SEM images are shown in figures 2(a) and (b), respectively. The NW growth direction is indicated by the arrow pointing towards the tip. The spatial variation of the CL emission for the structures with [N] = 0.08% and 0.12% in terms of spectral position and intensity are shown in figures 2(c) and (d), respectively. The CL maps were obtained at 8 K by scanning the electron beam along the NW axis. One should note that the intensity variation is plotted on a logarithmic axis as the variations along the nanowire can be more than two orders of magnitude. The CL spectra depicted in figures 2(e) and (f) were acquired from the spatial positions marked in figures 2(a) and (b). By examining the CL data from the NW with [N] = 0.08% in figures 2(c) and (e), a strong shift of the CL spectra along the NW axis is clearly seen. Furthermore, an apparent correlation between the CL spectral position and its intensity is observed, where the CL emission in the red is accompanied by a decrease in its intensity by up to three orders of magnitude. We compared the spatially dependent CL (figures 2(c) and (e)) and the TEM (figure 1(a)) data for the NW with 0.08% of nitrogen, and found that the red shift and reduction of the CL intensity both occur in the areas with a high density of structural defects. Surprisingly, this behavior is much less pronounced in the NWs with a higher nitrogen content of 0.12% (figures 2(d) and (f)), where the CL spectral position remains almost constant along the NW. In addition, the spatial variations of the CL intensity remain below one order of magnitude.

The effect of the N content on the PL properties was also examined by using μPL spectroscopy with varying laser excitation power (W_{exc}). The corresponding results from the representative GaNAsP NWs with [N] = 0.08% and 0.12% are shown in figures 3(a) and (b), respectively. In both NW structures the spectra contain two contributions: a broad and asymmetric PL band with a long low-energy tail and a series of sharp lines. Increasing nitrogen content causes an overall red shift of the PL spectra, expected from the bandgap reduction induced by the N. The decrease in the bandgap energy reflects the giant bandgap bowing characteristic for dilute nitrides and is caused by the anticrossing interaction between the localized nitrogen state and the extended conduction band states [31, 41]. The broad PL component can be attributed to radiative recombination of excitons weakly localized within band-tail states, formed by long-range

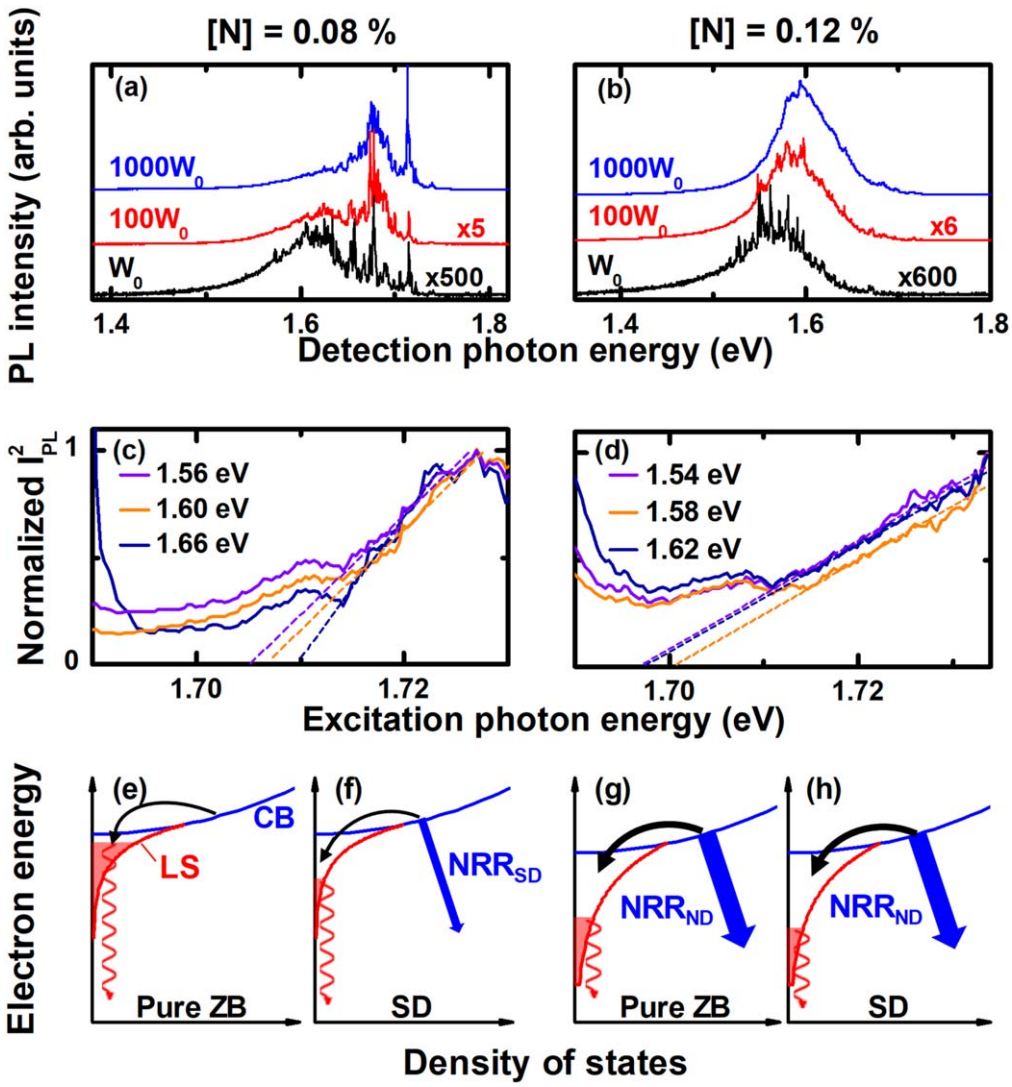

Figure 3. μPL spectra acquired at varying laser powers from the representative GaNAsP NWs with [N] = 0.08% (a) and 0.12% (b). W_0 denotes the lowest power of 2 μW μm^{-2} used during the measurements. (c) and (d) show the corresponding μPLE spectra acquired at three different detection energies of the LE emission. The PLE spectra are normalized to the same maximum intensity. The dashed lines in (c) and (d) are linear fits to the onset of the band-to-band transition in the PLE spectra. (e)–(h) Schematic illustration of DOS for the conduction band (CB) states and localized states (LS) together with the dominant recombination and capture processes in the areas with low (labeled as pure ZB) and high density of structural defects (SD). The shaded areas illustrate filling of the LS. The wavy red arrows indicate the LE emission detected in the CL and PL experiments. The straight blue arrows represent non-radiative (NR) recombination related to structural defects (NRR_{SD}) or other N-induced defects (NRR_{ND}) that are not caused by twinning. The curved black arrows show trapping of the generated electrons by the LS. The arrow thicknesses scale with efficiency of the corresponding processes.

fluctuations of the nitrogen content [40]. Such localized exciton (LE) emission typically governs radiative recombination in dilute nitrides at low temperatures [31, 43], and has an asymmetric lineshape, with the low-energy tail representing the statistical distribution of the band-tail states. This asymmetry is somewhat less pronounced in the CL spectra, which can be attributed to a much smaller excitation volume such that the sampling is highly local and non-statistical. The sharp lines superimposed on the broad LE band, which are also seen in the CL spectra, are most likely due to recombination of highly-localized excitons trapped within QD-like states (or N-cluster states) formed by short-range N fluctuations. Similar sharp lines were detected previously in low-temperature PL spectra of GaNAs NWs [44, 45]. These lines are beyond the scope of the present paper and will therefore not be discussed further. In the GaNAsP NWs with [N] = 0.08%, increasing W_{exc} causes a blue shift of the LE emission due to filling of the localized states—see figure 3(a). Moreover, the μPL spectrum measured under the highest W_{exc} of 2 mW m^{-2} shifts to similar energies as that of the CL emission detected from the area with a low density of structural defects. This suggests that the steady-state density of carriers/excitons generated by the electron beam in CL is higher, likely due to a higher excitation power density. A blue shift of the PL spectra with increasing W_{exc}, however, is not pronounced in the NWs with the higher N content of 0.12%, implying that the localized states are not filled under the utilized W_{exc}.

In order to understand these results, we first discuss the origin of spatial non-uniformity of the CL emission in the NWs containing 0.08% of nitrogen (figures 2(c), (e)). It could reflect changes in the alloy composition along the NW: the NW areas with a higher average N content would emit light at longer wavelengths. The gradient in the density of structural defects may favor a compositional inhomogeneity in both groups of NWs (0.08% and 0.12% N). This scenario can be cross-checked by utilizing μPLE spectroscopy. Indeed, μPLE spectra of the LE emission are dominated by optical transitions via surrounding extended states that have a higher density-of-states (DOS). Therefore, the bandgap energies can be found from the intercept with the x-axis of the linear fit (shown by the dashed lines) to the high-energy part of the PLE spectra displayed in the coordinate of I_{PL}^2 versus E_{exc}. Here I_{PL} is the detected PL intensity and E_{exc} is the excitation photon energy. The corresponding results from the representative GaNAsP NWs with [N] = 0.08% are shown in figure 3(c). Apparently, the bandgap energies computed from the three different PLE curves differ very little, by about 5 meV, for the detection energies ranging between 1.56 and 1.66 eV. This means that the alloy content is uniform throughout the NW, since the low and high-energy parts of the PL spectrum mainly originate from the areas with the high and low defect densities, respectively. Both of these areas are simultaneously excited during the μPL measurements due to a large excitation spot (approximately 1 μm). Therefore, we can rule out changes in the alloy composition as the origin of the spatial variation in the CL spectra.

Alternatively, the observed energy shift and intensity decrease of the CL emission in the areas with the high stacking-fault density could be caused by an increasing contribution of NR recombination in the vicinity of the structural defects. Indeed, several studies have concluded SF in III–V NWs have a detrimental effect on the overall emission efficiency, evident from a reduction of non-equilibrium carrier lifetime [19–23]. In dilute nitrides, the increasing NR recombination could also cause a red shift of the LE emission as filling of the localized states depends on the density of generated non-equilibrium carriers/excitons, which will be reduced under the influence of efficient NR recombination. The increasing NR recombination in the areas with more structural defects in the GaNAsP NWs with [N]=0.08% can leave the higher-energy LEs unpopulated, leading to the observed lower energy of the LE emission, as schematically illustrated in figures 3(e) and (f). Vice versa, increasing density of the generated carriers due to e.g. suppressed NR recombination or increased W_{exc} should lead to a blue shift of the emission, consistent with the CL and μ-PL data (figures 2(b) and 3(a)). Based on these results we attribute the non-uniformity in the CL properties of the GaNAsP NWs with 0.08% of nitrogen to the presence of structural defects that either directly act as NR recombination centers or promote formation of other NR point defects in their vicinity.

Though the density and distribution of the structural defects do not change significantly with increasing N content, see figure 1, the CL emission is more spatially homogeneous in the GaNAsP NWs with [N] = 0.12% (figures 2(d), (f)),

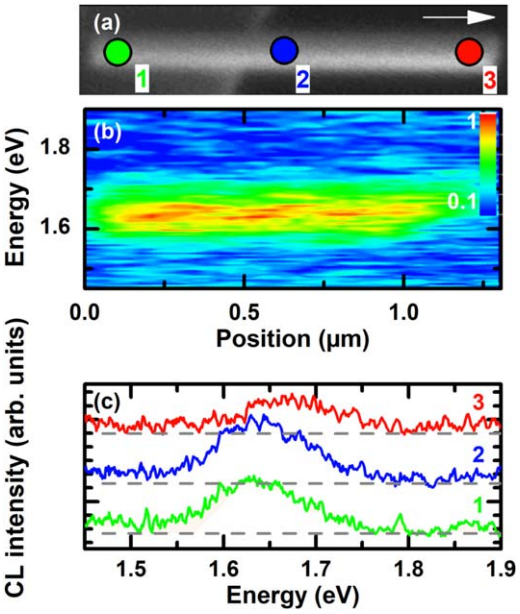

Figure 4. SEM image (a) together with spatial and spectral distributions of the CL emission (b) measured at 300 K using an acceleration voltage of 2 kV, from a representative GaNAsP NW with [N] = 0.08%. The CL image in (b) is displayed in the logarithmic scale. (c) CL spectra acquired from several spatial locations marked in (a). The spectra are displayed in the linear scale and vertically offset, for clarity.

both in terms of the emission energy and its intensity. There appears to be no correlation between them and the distribution of the structural defects. This observation could imply that NR recombination via structural defects can no longer compete with other more efficient channels responsible for capture and recombination of generated carriers/excitons. The latter include more efficient NR point defects [46–48] facilitated by N incorporation and faster trapping to the localized states, provided that the density of such localized states is higher in the NWs with [N] = 0.12%—see figures 3(g) and (h) for a schematic illustration of the proposed model. This is indeed consistent with the results of the power-dependent μPL measurements (figure 3(b)), which shows that in this structure increasing W_{exc} no longer results in filling of the localized states due to e.g. their higher density, in sharp contrast to the results for the NWs with the lower N content discussed above. Moreover, the localization energy increases from 47 ± 12 to 59 ± 9 meV when the nitrogen content increases from 0.08% to 0.12%. (These values represent mean values estimated from the slope of the low-energy PL tail for several NWs from each structure). We, therefore, suggest that owing to increased localization and formation of other N-induced defects (not related to twinning), structural defects no longer dominate in carrier recombination in the NWs with the higher [N]. We note that the nitrogen distribution remains homogeneous even in the NWs with 0.12% of nitrogen as evident from the results from the μPLE measurements shown in figure 3(d).

Finally, we investigate effects of the revealed structural defects on optical properties of these structures at room temperature (RT). Figure 4 shows spatial distributions of the

CL intensity and energy measured from a representative GaNAsP NW with 0.08% of N. Both the emission energy and intensity become more homogeneous at RT, in contrast to the low-temperature data in figures 2(c) and (e). The observation of the homogeneous emission energy further supports the absence of gradients in the nitrogen composition between the ends to the center of the NWs, as also observed at low temperature by μPLE spectroscopy (figure 3(c)). Indeed, at RT thermal depopulation of the localized states leads to predominance of free carrier/exciton emission [40], as is also evident from the fact that the peak position of the detected emission closely corresponds to the bandgap energy calculated using the band anticrossing model [41]. Interestingly, the emission intensity does not vary much along the NW, despite the presence of structural defects. The same behavior is also observed for the NWs with 0.12% N (see supporting information). This suggests that these defects, though important at low temperatures, do not dictate carrier recombination at RT, which is now governed by other NR channels, e.g. surface states. The same trend was reported previously for GaNP NWs [49].

4. Conclusions

In conclusion, we investigated the effects of structural defects on carrier recombination in GaNAsP NWs with two different N compositions. It is found at low N content and low temperatures these defects promote efficient NR recombination, either directly or indirectly. This leads to a large spatial inhomogeneity of the emission characteristics, both in terms of emission intensity and energy, in the NWs with the lower N content. These detrimental effects can be suppressed by even a small increase in nitrogen composition from 0.08% to 0.12%. This is attributed to more efficient trapping of excited carriers/excitons to the localized states promoted by N-induced localization and also to the presence of other NR channels. At RT, the structural defects no longer influence the carrier recombination even in NWs with lower nitrogen content. This finding points out that other NR defects, most likely point or surface defects, whose formation is insensitive to the occurrence of structural defects, are the dominant NR recombination centers as they are thermally activated much more strongly than the structural defects. Our work thus calls for future research efforts in identifying and eliminating these important NR centers in GaNAsP NWs, in order to fully explore potential applications of such NWs in nanoscale optoelectronic devices.

Acknowledgments

Financial support by Linköping University through the Professor Contracts, the Swedish Research Council (Grant No. 2016-05091), the Swedish Energy Agency (Grant No. P40119-1) and the Swedish Government Strategic Research Area in Materials Science on Functional Materials at Linköping University (Faculty Grant SFO-Mat-LiU No 2009 00971) is greatly appreciated. AFiM and LF thank funding from the Swiss National Foundation through the NCCR QSIT.

ORCID iDs

Mattias Jansson https://orcid.org/0000-0001-5751-6225
Jan E Stehr https://orcid.org/0000-0001-7640-8086
Anna Fontcuberta I Morral https://orcid.org/0000-0002-5070-2196

References

[1] Li Y, Qian F, Xiang J and Lieber C M 2006 Nanowire electronic and optoelectronic devices *Mater. Today* **9** 18
[2] Yan R, Gargas D and Yang P 2009 Nanowire photonics *Nat. Photon.* **3** 569
[3] Joyce H J *et al* 2011 III–V semiconductor nanowires for optoelectronic device applications *Prog. Quantum Electron.* **35** 23
[4] Huang M H, Mao S, Feick H, Yan H, Wu Y, Kind H, Weber E, Russo R and Yang P 2001 Room-temperature ultraviolet nanowire nanolasers *Science* **292** 1897
[5] Duan X, Huang Y, Agarwal R and Lieber C M 2003 Single-nanowire electrically driven lasers *Nature* **421** 241
[6] Saxena D, Mokkapati S, Parkinson P, Jiang N, Gao Q, Tan H H and Jagadish C 2013 Optically pumped room-temperature GaAs nanowire lasers *Nat. Photon.* **7** 963
[7] Tchernycheva M *et al* 2014 Integrated photonic platform based on InGaN/GaN nanowire emitters and detectors *Nano Lett.* **14** 3515
[8] Bermúndez-Ureña E, Tutuncuoglu G, Cuerda J, Smith C L C, Bravo-Abad J, Bozhevolnyi S I, Fontcuberta I Morral A, Carcía-Vidal F J and Quidant R 2017 Plasmonic waveguide-integrated nanowire laser *Nano Lett.* **17** 747
[9] Sirbuly D J, Tao A, Law M, Fan R and Yang P 2007 Multifunctional nanowire evanescent wave optical sensors *Adv. Mater.* **19** 61
[10] Dick K A, Caroff P, Bolinsson J, Messing M E, Johansson J, Deppert K, Wallenberg L R and Samuelson L 2010 Control of III–V nanowire crystal structure by growth parameter tuning *Semicond. Sci. Technol.* **25** 024009
[11] Johansson J, Karlsson L S, Dick K A, Bolinsson J, Wacaser B A, Deppert K and Samuelson L 2009 Effects of supersaturation on the crystal structure of gold seeded III–V nanowires *Cryst. Growth Des.* **9** 766
[12] Spirkoska D *et al* 2009 Structural and optical properties of high quality zinc-blende/wurtzite GaAs nanowire heterostructures *Phys. Rev.* B **80** 245325
[13] Vainorius N, Jacobsson D, Lehmann S, Gustafsson A, Dick K A, Samuelson L and Pistol M-E 2014 Observation of type-II recombination in single wurtzite/zinc-blende GaAs heterojunction nanowires *Phys. Rev.* B **89** 165423
[14] Belabbes A, Panse C, Furthmüller J and Bechstedt F 2012 Electronic bands of III–V semiconductor polytypes and their band alignment *Phys. Rev.* B **86** 075208
[15] Pemasiri K *et al* 2009 Carrier dynamics and quantum confinement in type II ZB-WZ InP nanowire homostructures *Nano Lett.* **9** 648
[16] Jahn U, Lähnemann J, Pfüller C, Brandt O, Breuer S, Jenichen B, Ramsteiner M, Geelhaar L and Riechert H 2012 Luminescence of GaAs nanowires consisting of wurtzite and zinc-blende segments *Phys. Rev.* B **85** 045323

[17] Vainorius N, Lehmann S, Jacobsson D, Samuelson L, Dick K A and Pistol M-E 2015 Confinement in thickness-controlled GaAs polytype nanodots *Nano Lett.* **15** 2652

[18] Akopian N, Patriarche G, Liu L, Harmand J-C and Zwiller V 2010 Crystal phase quantum dots *Nano Lett.* **10** 1198

[19] Perera S *et al* 2008 Nearly intrinsic exciton lifetimes in single twin-free GaAs/AlGaAs core–shell nanowire heterostructures *Appl. Phys. Lett.* **93** 053110

[20] Woo R L, Xiao R, Kobayashi Y, Gao L, Goel N, Hudait M K, Mallouk T E and Hicks R F 2008 Effect of twinning on the photoluminescence and photoelectrochemical properties of indium phosphide nanowires grown on silicon (111) *Nano Lett.* **8** 4664

[21] Parkinson P, Joyce H J, Gao Q, Tan H H, Zhang X, Zou J, Jagadish C, Herz L M and Johnston M B 2009 Carrier lifetime and mobility enhancement in nearly defect-free core–shell nanowires measured using time-resolved terahertz spectroscopy *Nano Lett.* **9** 3349

[22] Sourribes M J L, Isakov I, Panfilova M, Liu H and Warburton P A 2014 Mobility enhancement by Sb-mediated minimization of stacking fault density in InAs nanowires grown on silicon *Nano Lett.* **14** 1643

[23] Zhou X, Lu M-Y, Lu Y-J, Jones E J, Gwo S and Gradečak S 2015 Nanoscale optical properties of indium gallium nitride/gallium nitride nanodisk-in-rod heterostructures *ACS Nano* **9** 2868

[24] Glas F, Harmand J-C and Patriarche G 2007 Why does wurtzite form in nanowires of III–V zinc blende semiconductors? *Phys. Rev. Lett.* **99** 146101

[25] Joyce H J, Gao Q, Tan H H, Jagadish C, Kim Y, Zhang X, Guo Y and Zou J 2007 Twin-free uniform epitaxial GaAs nanowires grown by a two-temperature process *Nano Lett.* **7** 921

[26] Dick K A, Thelander C, Samuelson L and Caroff P 2010 Crystal phase engineering in single InAs nanowires *Nano Lett.* **10** 3494

[27] Joyce H J, Wong-Leung J, Gao Q, Tan H H and Jagadish C 2010 Phase perfection in zinc blende and wurtzite III–V nanowires using basic growth parameters *Nano Lett.* **10** 908

[28] Ahtapodov L, Todorovic J, Olk P, Mjåland T, Slåttnes P, Dheeraj D L, van Helvoort A T J, Fimland B-O and Weman H 2012 A story told by a single nanowire: optical properties of wurtzite GaAs *Nano Lett.* **12** 6090

[29] Conesa-Boj S, Kriegner D, Han X-L, Plissard S, Wallart X, Stangl J, Fontcuberta I Morral A and Caroff P 2014 Gold-free ternary III–V antimonide nanowire arrays on silicon: twin-free down to the first bilayer *Nano Lett.* **14** 326

[30] Jacobsson D, Panciera F, Tersoff J, Reuter M C, Lehmann S, Hofmann S, Dick K A and Ross F M 2016 Interface dynamics and crystal phase switching in GaAs nanowires *Nature* **531** 317

[31] For a review on dilute nitrides, see e.g. Buyanova I A and Chen W M 2004 *Physics and Applications of Dilute Nitrides* (New York: Taylor and Francis)

[32] Kudrawiec R, Luce A V, Gladysiewicz M, Ting M, Kuang Y J, Tu C W, Dubon O D, Yu K M and Walukiewicz W 2014 Electronic band structure of $GaN_xP_yAs_{1-x-y}$ highly mismatched alloys: suitability for intermediate-band solar cells *Phys. Rev. Appl.* **1** 034007

[33] Jussila H, Kivisaari P, Lemettinen J, Tanaka T and Sopanen M 2015 Two-photon absorption in $GaAs_{1-x-y}P_yN_x$ intermediate-band solar cells *Phys. Rev. Appl.* **3** 054007

[34] Suemune I, Uesugi K and Walukiewicz W 2000 Role of nitrogen in the reduced temperature dependence of band-gap energy in GaNAs *Appl. Phys. Lett.* **77** 3021

[35] Wang X J, Buyanova I A, Zhao F, Lagarde D, Balocchi A, Marie X, Tu C W, Harmand J C and Chen W M 2009 Room-temperature defect-engineered spin filter based on a non-magnetic semiconductor *Nat. Mater.* **8** 198

[36] Puttisong Y, Wang X J, Buyanova I A, Geelhaar L, Riechert H, Ptak A J, Tu C W and Chen W M 2013 Efficient room-temperature nuclear spin hyperpolarization of a defect atom in a semiconductor *Nat. Commun.* **4** 1751

[37] Puttisong Y, Buyanova I A, Ptak A J, Tu C W, Geelhaar L, Riechert H and Chen W M 2013 Room-temperature electron spin amplifier based on Ga(In)NAs alloys *Adv. Mater.* **25** 738

[38] Chen S, Huang Y, Visser D, Anand S, Buyanova I A and Chen W M 2018 Room-temperature polarized spin-photon interface based on a semiconductor nanodisk-in-nanopillar structure driven by few defects *Nat Commun.* **9** 3575

[39] La R, Pan J L, Bastiman F and Tu C W 2016 Self-catalyzed Ga(N)AsP nanowires and GaAsP/GaNAsP core–shell nanowires grown on Si(111) by gas-source molecular beam epitaxy *J. Vac. Sci. Technol.* B **34** 02L108

[40] Jansson M, Chen S, La R, Stehr J E, Tu C W, Chen W M and Buyanova I A 2017 Effects of nitrogen incorporation on structural and optical properties of GaNAsP nanowires *J. Phys. Chem.* C **121** 7047

[41] Shan W, Walukiewicz W, Ager J W III, Haller E E, Geisz J F, Friedman D J, Olson J M and Kurtz S R 1999 Band anticrossing in GaInNAs alloys *Phys. Rev. Lett.* **82** 1221

[42] Vurgaftman I and Meyer J R 2003 Band parameters for nitrogen—containing semiconductors *J. Appl. Phys.* **94** 3675

[43] Buyanova I A, Chen W M, Pozina G, Bergman J P, Monemar B, Xin H P and Tu C W 1999 Mechanism for low-temperature photoluminescence in GaNAs/GaAs structures grown by molecular-beam epitaxy *Appl. Phys. Lett.* **75** 501

[44] Filippov S, Jansson M, Stehr J E, Palisaitis J, Persson P O Å, Ishikawa F, Chen W M and Buyanova I A 2016 Strongly polarized quantum-dot-like light emitters embedded in GaAs/GaNAs core/shell nanowires *Nanoscale* **8** 15939

[45] Jansson M, Ishikawa F, Chen W M and Buyanova I A 2018 N-induced quantum dots in GaAs/Ga(N, As) core/shell nanowires: symmetry, strain and electronic structure *Phys. Rev. Appl.* **10** 044040

[46] Buyanova I A, Chen W M and Tu C W 2004 Defects in dilute nitrides *J. Phys.: Condens. Matter.* **69** 201303

[47] Li W, Pessa M, Ahlgren T and Decker J 2001 Origin of improved luminescence efficiency after annealing of Ga(In) NAs materials grown by molecular-beam epitaxy *Appl. Phys. Lett.* **79** 1094

[48] Toivonen J, Hakkarainen T, Sopanen M, Lipsanen H, Oila J and Saarinen K 2003 Observation of defect complexes containing Ga vacancies in GaAsN *Appl. Phys. Lett.* **82** 40

[49] Dobrovolsky A, Persson P O Å, Sukrittanon S, Kuang Y, Tu C W, Chen W M and Buyanova I A 2015 Effects of polytypism on optical properties and band structure of individual Ga(N)P nanowires from correlative spatially resolved structural and optical studies *Nano Lett.* **15** 4052